ADAPTATION OF THE ESPSS/ECOSIMPRO PLATFORM FOR THE DESIGN AND ANALYSIS OF LIQUID PROPELLANT ROCKET ENGINES

J. Amer[(1)], J. Moral[(2)], J.J. Salvá[(3)]

(1) Final thesis. Departamento de Motopropulsion y Termofluidodinámica, E.T.S. Ingenieros Aeronáuticos, Universidad Politécnica de Madrid (*email: pepamer@gmail.com*)
(2) Empresarios Agrupados Internacional. S.A. Magallanes, 3. 28015 Madrid. Spain. *(email: frj@empre.es)*
(3) Departamento de Motopropulsion y Termofluidodinámica, E.T.S. Ingenieros Aeronáuticos, Universidad Politécnica de Madrid. Pza. del Cardenal Cisneros, 3. 28040 Madrid. Spain *(email: josej.salva@upm.es)*

Abstract

The preliminary design of rocket engines has been historically a semi-manual process, where the specialists work out a start point for the next design steps. Thanks to the capabilities of the EcosimPro language, such as non causal programming, a natural pre-design model has been physically discomposed in three modules: propulsion performance, sizing and mass, and mission requirements. Most of the new stationary capabilities are based on the ESPSS libraries, which are able to simulate in great detail transient phenomena of fluid systems (e.g. tanks, turbomachinery, nozzles and combustion chambers).

Once the base of the three pre-design modules is detailed, an effort has been made to determine accurately the mission requirements. For example, in a geostationary transfer orbit insertion maneuver, the maximum change of speed is obtained considering a finite combustion, instead of the ideal Hohmann transfer orbit.

Finally, the model validation and two application examples are presented: the first one compares the model results with the real performance of the Aestus pressurized rocket engine. In the second one, the relation between the initial total vehicle mass and the design parameters (combustion pressure, mixture ratio and nozzle area ratio) is obtained, looking for an optimized pre-design. And the last one, take advantage of the ESPSS transient capabilities simulating a transient engine run (startup, maneuver and shutdown), which is used as simplified analysis to verify the optimum pre-design.

1. INTRODUCTION

The state of the art in preliminary design of liquid propellant rocket engines was developed by Manski in the late 80's (see [3]). The scheme in *Figure 1* sums up the sequential process to obtain a particular engine pre-design, given the cycle specifications and the mission requirements.

The main goal is to get the design of a liquid propellant rocket engine. Then, given the following "input" data:

- Mission requirements: payload mass, vehicle change of speed and maximum acceleration,
- Cycle specifications: propellants, combustion and expansion efficiency, pressure losses,

the developed modules are able to determine the engine "sizing", represented by:

- Design parameters: chamber pressure (p_c), mixture ratio (MR), and expansion area ratio (ε_e)
- Propulsion characteristics (I_{sp}, c^*, c_F)
- Sizing and mass (throat diameter, thrust, propellants mass, etc.)

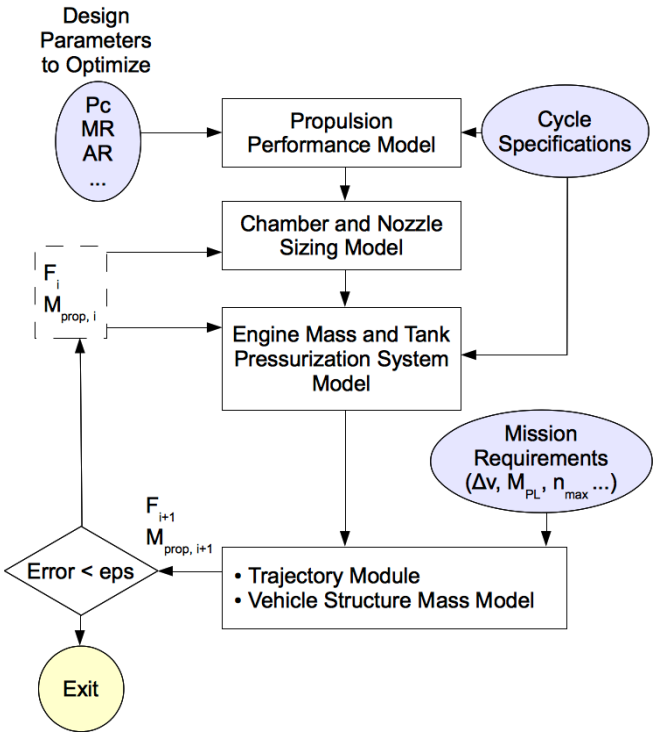

Figure 1. Preliminary design methodology

The value of the design parameters is obtained as a result of an optimization procedure. That is, the preliminary design is based on the optimum condition (minimum initial vehicle mass) and the appropriate boundary conditions (engine diameter limited by the spacecraft cowling size). As consequence, the more design parameters are selected, the more freedom degrees has the rocket preliminary design.

After iterating in the design parameters, a minimum mass is reached, and so, the optimum preliminary design point. Once the design parameters are obtained as a result of the optimization, propulsion characteristics, geometry and mass of the liquid propellant rocket engine are directly determined by the presented scheme (*Figure 1*).

All the models have been written on EcosimPro (see [1]), which is a powerful tool modeling physical systems represented by differential-algebraic equations (DAE). The final model iterating in the

design parameters is also *automatically* built by EcosimPro and coupled to an external optimizer, which is run from the EcosimPro environment.

Some of the new stationary models are based on the ESPSS libraries, which are an initiative of the European Space Agency to create a European simulation platform for spacecraft and launcher propulsion systems (see [2]). Its rigorous models of fluid properties and chemical equilibrium guarantee a proper base for the preliminary design.

2. PRELIMINARY DESIGN METHODOLOGY

Thanks to the non causal EcosimPro Language, the sequential and rigid model presented in *Figure 1* have been simplified and structured in three separated modules: combustor chamber and nozzle; Sizing and Mass; and Trajectory. Then, changes or improvements on a particular physical model would be easily reused by the global iterative process, due to an automatic mathematical model generation.

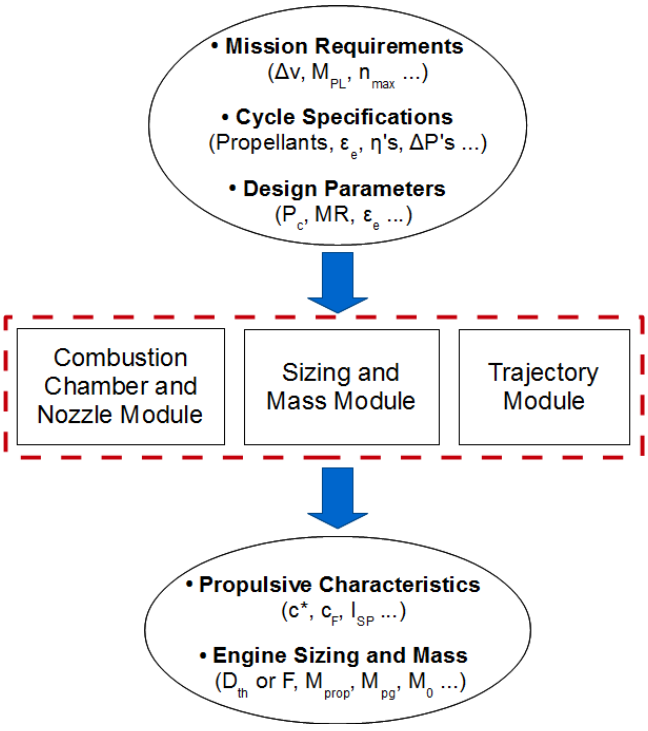

Figure 2. Applied modular methodology

In the following sections, the entry parameters and the three modules formulation are explained in detail.

3. MISSION REQUIREMENTS & CYCLE SPECIFICATIONS

Such as important as the preliminary design modules are the entry parameters, which are composed by the mission requirements and the cycle specifications. Remember that the design parameters (p_c, MR, ε_e) are determined as a result of the optimization.

A) Mission Requirements

As its name describes, the mission requirements define the mission goal, which is expressed by the maximum change of speed, Δv, and the payload mass, M_{PL}. Moreover, the lower limit of the maximum acceleration is given to fulfill the trajectory in accordance with a given Δv.

When the burning time is finite, that is, not instantaneous, the general rocket equation is expressed as follows (see [9]):

$$\Delta v^* = I_{sp} \ln \frac{M_0}{M_0 - M_{prop}} - \int_{t_1}^{t_2} g \cdot \sin\gamma \cdot dt$$

In order to harmonize the complexity of each module, the Tsiolkosky rocket equation is programmed in the trajectory module as a simplified version of the general rocket equation. Since the applied rocket equation in the trajectory module is simpler, the gravitational component is taken into account as *k* times·*Δv*, where *k* is a constant for each kind of maneuver:

$$\Delta v^* \cdot (1+k) = \Delta v = I_{sp} \ln \frac{M_0}{M_0 - M_{prop}}$$

The gravitational factor, *k*, can be determined through: historical/empirical values (see Fig. 6.12 at [9]), an analytical resolution of the trajectory, or an iterative process with different *k* values until the desired orbit height is reached. The last solution is selected because combines proper approximation level with low working time.

A new EcosimPro model called momentum, has been programmed in order to determine the vehicle trajectory based on the differential orbital mechanics formulation:

$$m \cdot \vec{a} = \vec{F}_{grav} + \vec{F}_{thrust}$$

The required data is: the initial vehicle mass, M_0; the angles between the thrust and velocity vectors, φ and θ; the earth radius; the earth gravitational parameter; and the initial circular orbit height. Moreover, the entry port gives information about the engine thrust and mass flow.

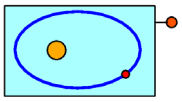

Figure 3. Symbol of the momentum component

Once the initial and final orbit are known, the gravitational factor, *k*, can be determined with the presented component. In the applied case, a typical perigee maneuver with NTO/MMH propellant combination results a gravitational factor of 0.035.

Finally, the maximum acceleration presents two limits as a result of a physical analysis:

- Upper limit: is fixed by the maximum stress that the vehicle structure and payload can withstand
- Lower limit: lets reach the final orbit height with a given Δv

In the first stage of a launch sequence, the upper limit of n_{max} usually applies because the axial and the lateral loads are dominant. Otherwise, in the perigee maneuvers the lower limit of n_{max} is given as an

historical parameter, which is a relation between the thrust and the final vehicle mass.

B) Cycle Specifications

These parameters are usually assigned by historical data or the experience of specialists. It lets determine the influence of the engine characteristics at the global performances (e.g. turbomachinery efficiency, propellant combination, pressure loss at ducts).

4. COMBUSTION CHAMBER AND NOZZLE MODULE

In order to determine the specific impulse from the propellant properties at the injection plate, some hypothesis must be applied. The thermodynamic process of vaporisation, mixing and reaction through the cylindrical combustion chamber is supposed to be isenthalpic but not isentropic. That is, no heat transfer through the walls is considered and the fluid acceleration is caused by a pressure loss:

$$h_{t,2} = h_{t,1}$$

$$P_2 = P_1 - \rho_2 \cdot v_2^2$$

On the other hand, the thermodynamic process in the nozzle from chamber exit to nozzle exit, is supposed to be isenthalpic and isentropic. That is, no heat transfer through the walls is considered, and the reacting flow model is either chemical shifting equilibrium or frozen flow, depending on the selected propellant combination.

$$h_{t,throat} = h_{t,exit} = h_{t,2}$$

$$s_{throat} = s_{exit} = s_2$$

For example, the characteristic combustion time of LH&LOX propellant combination is usually lower than the residence time, so that the chemical shifting equilibrium applies.

This combustion model is successfully represented by the previous four engine sections. In the case that heat transfer to the walls was considered, a deeper discretisation would be needed. Then the appropriate reacting flow model has to be selected in each one of the three existing volumes.

Once the fluid conditions at the injection plate are known, the fluid properties at the chamber exit, throat and nozzle exit are obtained by the following equation system:

$$y_{i,2}, T_2, s_2 = f_{\min Gibbs}(y_{i,inj}, h_{t,inj}, P_2, \frac{m_{cr}}{A_{th}}, \frac{A_{ch}}{A_{th}})$$

$$y_{i,th}, T_{th}, P_{th}, \frac{m_{cr}}{A_{th}} = f_{\min Gibbs}(y_{i,2}, h_{t,2}, s_2)$$

$$y_{i,exit}, T_{exit}, P_{exit} = f_{\min Gibbs}(y_{i,th}, h_{t,th}, s_{th}, \frac{m_{cr}}{A_{th}}, \frac{A_{ch}}{A_{th}})$$

With $i = 1, n_{products}$

Note that the model can be extended to a non-isentropic and non-isenthalpic process if the heat exchange through the walls is considered. It has been successfully proved in a testing model of an expander cycle with regenerative cooling.

Each one of these equation systems iterates in molar fractions, y_i; and temperature. Moreover, the complete module iterates in the pressure at the chamber exit, P_2; and in the mass flow per throat area, m_{cr}/A_{th}.

Once the fluid properties at the nozzle exit are determined, the propulsive characteristics can be calculated. In particular, the specific impulse is expressed as follows:

$$I_{sp} = \eta_b \eta_e \left[v_{exit} + \frac{\varepsilon_e}{G_{cr}} (P_{exit} - P_{amb}) \right]$$

Moreover, this module gives a first sizing factor represented by the mass flow, $\dot{m}$, which is based on the thrust determined in the other modules. Finally, it is related with the throat area, A_{th}, as follows:

$$\dot{m} = \frac{F}{I_{sp}}; \quad A_{th} = \frac{\dot{m}}{G_{cr}}$$

The complete formulation of this module is included in a new EcosimPro component, called LRE_eq (Liquid Rocket Engine, equilibrium). The necessary data to run this component are the design parameters, the cycle specifications and a numeric initialization. In order to be able to connect this module with the others, it has two ports:

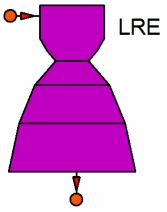

Figure 4. Symbol of the LRE_eq component

- Inlet port: it transfers the required thrust, and the propellants store conditions (T, P)
- Outlet port: it transfers the throat diameter, propellant combination, average nozzle pressure and the design parameters (p_c, MR, ε_e)

The obtained propulsion characteristics have been compared with:

- Real rocket engine performance: given the same thrust, propellant store conditions, design parameters and cycle specifications, the difference between the presented model and the nominal $I_{sp,vac}$ results less than 1.5%. The main reasons that justify this error are that the real expansion process is between the two reacting flow models (frozen or equilibrium), and that the combustion and expansion efficiencies have typical values, that is, not specific for each engine model
- CEA java application (see [4]): the calculated specific impulse is almost the same in both programs because they use the same chemical equilibrium model, based on the minimum Gibbs free energy. The main differences are that LRE_eq is more flexible and, for example, can model the finite

area combustor with chemical equilibrium until the nozzle throat. Moreover, the fluid properties data base in the ESPSS libraries lets calculate the propellant enthalpy until the injection plate based on real properties, that is, as a function of pressure and temperature. On the other hand, the calculated enthalpy of CEA java application is related to a specific temperature and pressure

5. SIZING AND MASS MODULE

The initial vehicle mass, M_0, and the propellant mass, M_{prop}, are decisive parameters on rocket performance, as the main goal is to elevate the maximum payload to a determinate orbit.

In order to determine the initial vehicle mass, the mass of all the engine components must be calculated. In the particular case of a pressured rocket engine, the initial mass of the propulsion system can be split up as:

$$M_{PS} = M_{engine} + M_{\tan k} + M_{prop} + M_{others}$$

In turn, the engine mass is discomposed in the injection system, combustion chamber and nozzle. Based on the structural material and on the design loads, the structural mass of each subcomponent is calculated.

In order to consider the secondary loads or additional components (e.g. regenerative circuit), it is necessary to apply a correction factor:

$$K_i = \frac{M_{i,real}}{M_{i,struc}}$$

For example, the injection head mass has been modeled as the set of three built-in circular plates, which main load is buckling. Assuming the Reissner-Mindlin and Kircchoff-love hypothesis of plate theory, the thickness of each plate can be formulated as follows:

$$t_{inj} = \sqrt{\frac{3 p_b D_c^2}{16 \sigma_u}}$$

Where p_b is the burst pressure, which is usually supposed to be twice the maximum expected working pressure, p_{MEW} (see [5] and [6]). On the other hand, σ_u is the ultimate tensile strength, and its value depends on the structural material. Finally, the structural mass of the injector head is 3 times the mass of one circular plate, which is obtained as the product of the material density and the structural volume:

$$M_{inj,struc} = 3 \rho_{inj} S_{inj} t_{inj}$$

Once the structural mass is calculated, it has to be multiplied with the appropriate correction factor in order to have a proper approximation of the injection head mass.

The grade of accuracy in the mass calculation strongly depends on the correction factor. In this study, it is the result of the comparative analysis between the real component mass of the HM-7B rocket engine and the structural mass based on the same materials and loads.

Component	Structural Model	Correction Factor, K_i
Combustion chamber	Circular built-in plates buckling	1.85
Nozzle	Thin plate theory	1.46
Injection system	Thin plate theory and minimum structural thickness	1.85

Since the combustion chamber and nozzle have to withstand the combustion pressure and the expansion pressure, the thin plate theory is used to determine the necessary thickness, and so, the mass of each component. Moreover, two parameters must be defined in the cycle specifications in order to determine the combustion chamber length, L_c, and the nozzle length, L_{nz}. That is, the value of the characteristic length, L*, and the fractional length, L_f, must be fixed as historical data.

Another possible approximation to determine the engine mass is through given correlations, as such the relation between the bi-propellant engine mass and the thrust presented in Humble [5]. As expected, this method is less accurate than the previous one, since it does not consider the material and the main loads.

In the same way, the mass of the propellant and pressurized gas tanks is approximated as a function of the material properties, the main load and the fluid volume. The structural thickness is calculated with the pressure vessel model, which lets determine the tank structural mass through the material density.

The respective correction factors have been determined for spherical propellant tanks and spherical pressurized gas tanks. In order to obtain these factors, the real mass of several spherical tanks has been compared with their structural mass. The result is a clear correlation between the correction factor and the tank volume for the propellant tanks, and a constant value for the pressurized gas tanks.

Component	Correction Factor, K_i
Propellant tank	$V<0.72m^3$: 2.4-1.6·V $V>0.72m^3$: 1.244
Pressurized gas tank	1.125

The propellant tank factor depends on the volume because the secondary tank components, such as the propellant management device and the tank valves, increase their mass contribution to the total tank mass as the tank size decreases.

The volume of the previous tanks depends on the propellant mass, M_{prop}, which is, in fact, one of the most important contributions to the total initial mass. The burnt propellant mass is calculated as the product of the reacting flow, $\dot{m}$, and the burning time, t_b:

$$M_{prop,b} = \dot{m} \cdot t_b$$

The burning time, t_b, is an independent variable of the global equation system.

In order to have in account the propellant percentage that is used to prime the ducts and the tank reserve, the propellant mass stored in the tanks is increased in 2% of $M_{prop,b}$. The oxidizer and reducer mass is function of the total propellant mass and the mixture ratio, *MR*:

$$M_{oxi} = \frac{MR}{1+MR} M_{prop}$$

$$M_{red} = \frac{1}{1+MR} M_{prop}$$

Finally, the oxidant and reducer volumes are based on their densities and stored mass. Moreover, it is necessary to consider some ullage, in order to guarantee the proper tank operation:

$$V_{\tan k,\, prop} = V_{prop} + V_{ullage} \quad with \quad V_{ullage} = 0.1 \cdot V_{\tan k,\, prop}$$

Once the propellant volume is known, the necessary pressurized gas volume to keep the propellant tank pressure at a constant value is calculated according to an adiabatic expansion process from the gas tank to the propellant tank (see [7]).

In M_{others} are included the pressurized-gas, the main propellant valves and miscellanies. In turn, the miscellanies are composed by ducts, regulator valves, secondary valves and filters. According to Manski, there is a correlation between the miscellanies mass and the engine thrust (see [8]), which is applied in this study.

6. TRAJECTORY MODULE

In order to have a complete equation system is necessary to add the trajectory requirements:

- Tsiolkovsky rocket equation: gives a relation between the maximum change of speed, the specific impulse (supposed constant during the burning), and the initial and final mass of the rocket. Knowing that the final rocket mass can be expressed as the difference between the initial rocket mass and the burned propellant mass, the equation is written as follows:

$$\Delta v = I_{sp} \ln \frac{M_0}{M_0 - M_{prop}}$$

- The total initial mass of the vehicle is the sum of the payload mass, M_{PL}, and the propulsion system mass, M_{PS}:

$$M_0 = M_{PL} + M_{PS}$$

  It is supposed that the mass of the payload and engine nacelles is included in the payload mass contribution.

- The maximum rocket acceleration, n_{max}, occurs at the end of the combustion process because the vehicle mass has its minimum. Considering a quasi-tangential trajectory and constant thrust, n_{max} is expressed as follows:

$$n_{\max} = \left(\frac{dv}{dt}\right)_{\max} = \frac{F}{M_0 - M_{prop}}$$

Once both, sizing and mass, and trajectory modules have been analyzed, the new EcosimPro component called LRE_PF_design is presented (Liquid Rocket Engine, Pressure-fed, design).

Two ports have been installed in order to connect this component with the LRE_eq component, so that the complete rocket engine model is solvable.

- Inlet port: it reads the throat diameter, propellant combination, average nozzle pressure and the design parameters (p_c, MR, ε_e)
- Outlet port: it transfers to LRE_eq the required thrust, and the propellants store conditions (T,P)

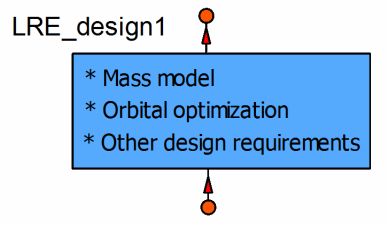

Figure 5. LRE_PF_design EcosimPro Component

Moreover, the following data must be given to the component

- Mission requirements: maximum change of velocity, payload mass and maximum acceleration
- The rest of the cycle specifications that have not been defined in the LRE_eq component. This data is related to the previous models, including material properties of the engine components (combustion chamber, nozzle, propellant and pressured-gas tanks) and main propellant valves' mass

7. MODEL VALIDATION

The complete model is composed by the two previous components, LRE_eq and LRE_PF_design, providing all the equations for the preliminary design of a pressurized rocket engine. That is, the propulsion characteristics and the sizing-and-mass of the pressurized engine are obtained for a given mission requirements, cycle specifications and design parameters.

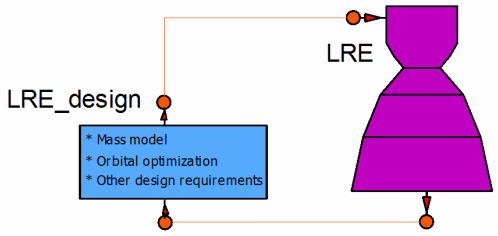

Figure 6. Complete Rocket Engine Model

EcosimPro is able to resolve jointly the three sub-models (combustion chamber and nozzle; sizing and mass; and trajectory). In order to solve this mathematical problem, EcosimPro does the following operations automatically:

- Classification of the three sub-models' equations

- Selection (assisted by the user) of the algebraic variables which are used to iterate. In our study, the three following variables are selected: critical mass flow and throat area ratio m/A_{th}, static pressure at combustion chamber exit p_2, and the burnt propellant mass M_{prop}
- Iterative calculation of the previous three unknowns by advanced Newton method

Perigee maneuver:

In order to show how to run the model and to demonstrate its approximation level, an example of a perigee maneuver based on the Ariane 5G is solved.

Once all the entry data are defined, the EcosimPro schematic of the complete preliminary design model can be run. The result is compared with the Aestus performance through a set of representative variables.

The values of the mission requirements and cycle specifications are taken from:

- Ariane 5G maneuver data (see [10]) and some additional approximations: the following table shows the values which have been applied to the model in order to define the desired maneuver:

Mission Requirements	
Max. change of speed, Δv	2527.17 m/s
Payload mass, M_{PL}	6640 kg
Maximum accel., n_{max}	0.38·g m/s^2

The maximum change of speed is determined with the previous correction factor, *k*, and the change of speed which is needed for a Hohmann or ideal transfer orbit:

$$\Delta v = (1+k)\cdot \Delta v^* = 2527.17 m/s$$

The payload mass is obtained directly from the Ariane user's manual as it is one of the most important performance data in aerospace. Finally, the lower limit of n_{max} is based on a nominal data of an Aestus previous version, which value is n_{max}^*=0.4. In order to determine the maximum acceleration at the Aestus nominal point, the following approximation has been done,

$$n_{\max}\cdot g_0 \propto \frac{\Delta v}{t_b}, \text{ that is,}$$

$$n_{\max} = \left(\frac{t_b^*\cdot n_{\max}^*}{\Delta v^*}\right)\frac{\Delta v}{t_b} = \left(\frac{810\cdot 0.4\cdot g}{2154}\right)\frac{2527}{1000} = 0.38\cdot g$$

- Pressurized upper stage engine (Aestus). Its performance data lets assign a value to the cycle specifications and design parameters:

Cycle Specifications	
Propellant combination	MMH/NTO
Combustion Chamber area ratio, ε_{ch}	2.38
Fuel temperature in the tank	300 K
Oxidant temperature in the tank	300 K
Pressurized-gas temperature	295 K

Design Parameters	
Injection pressure, P_1	11.4 bar
Mixture ratio, MR	2.05
Nozzle area ratio, ε_e	84

Moreover, some values of the cycle specifications refers to the physical engine process and are obtained from empirical data of the literature:

Model Parameters	
Fractional length, L_f	0.8
Characteristic length, L*	0.89 m
Combustion efficiency, η_b	0.98
Expansion efficiency, η_e [1]	f(L_f, AR_{sup})

The resulting rocket engine is detailed through the following variables:

Variable	Modeled	Real	Relative error (%)
Specific Impulse in the vacuum (m/s)	3143.5	3178.4	1.1
Throat diameter (m)	0.135	0.136	0.7
Propellant mass (kg)	9628	9700	0.74
Intial vehicle mass (kg)	17086	17540	2.6

As it can be seen in the previous table, the initial vehicle mass has the maximum relative error. That is because M_0 accumulates each of its components' error. Since the values of the relative errors are low, the preliminary design model results a representative approximation as a first step in a full design sequence:

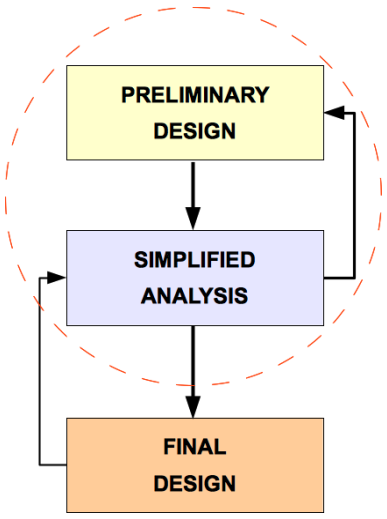

Figure 7. Complete design scheme

[1] The expansion efficiency is included in the model code as a empirical correlation

8. APPLICATION EXAMPLES

A) Preliminary design of a pressurized rocket engine

Focused on the same perigee maneuver, the preliminary design looks for the best design variables' combination, which minimizes the engine system mass.

On one hand, it is interesting to see the mass tendency with each one of the design parameters (P_1, MR and ε_e), while the other two are considered constant at the nominal value. Moreover, the cycle specifications and mission requirements have the same value as the previous application example.

Starting with the injection pressure, P_1, the following figure represents the initial mass variation while the mixture ratio and nozzle area ratio are fixed.

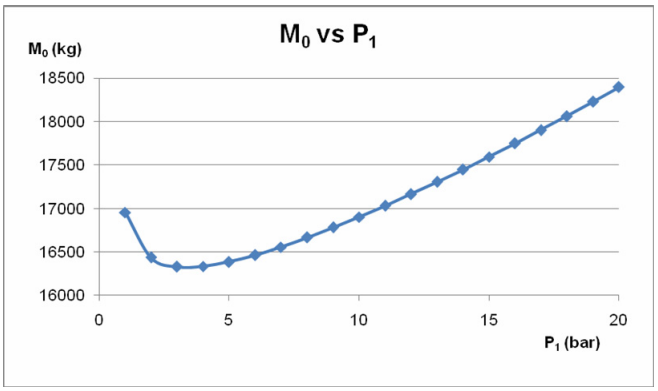

Figure 8. Initial vehicle mass as a function of the pressure at the injection section, considering nominal values of mixture ratio and nozzle area ratio

The optimized injection pressure, P_1, is 3.5 bar, which in fact, is much lower than the nominal Aestus P_1 (11.4 bar). The selection of a higher pressure can be due to:

- A geometric limitation factor: the higher the chamber pressure is, the smaller the rocket engine can be
- To avoid the cavitation of the regenerative circuit. The mass flux falls proportionally with lower pressure, while the heat flux through the walls has a slower decrease with lower pressure. Then a higher temperature is reached in the regenerative circuit with lower P_1. Finally, higher pressures are desired in order to avoid cavitations
- A good combustion stability caused by a higher pressure

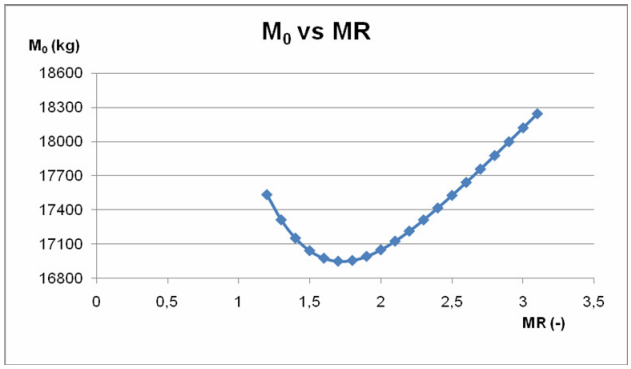

Figure 9. Initial vehicle mass as a function of the mixture ratio (nominal injection pressure and nozzle area ratio)

The optimized mixture ratio, MR, has a value of 1.7, while the Aestus nominal MR is 2.05. The minimum mass point corresponds to the maximum specific impulse, which in fact, depends on the propellant combination and the mixture ratio.

With the applied model hypothesis related to the propulsive characteristics (frozen flow from the throat, for MMH/NTO), it results the previous I_{sp} maximum. The historical MR data for the MMH/NTO propellant combination is between 1.65 and 2.05, which includes the previous optimized MR.

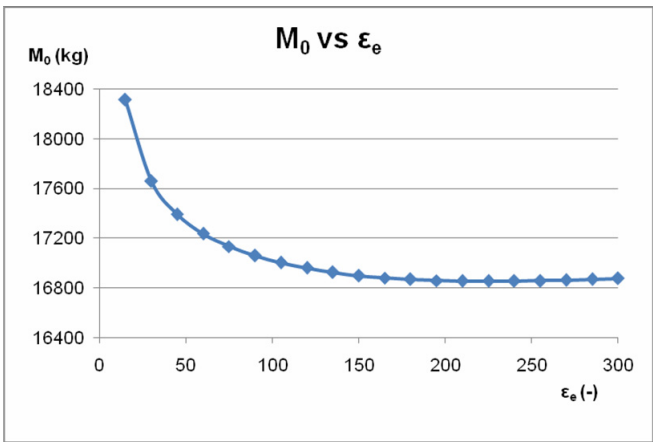

Figure 10. Initial vehicle mass as a function of nozzle area ratio, considering nominal values of the pressure at the injection section and mixture ratio

The optimized nozzle area ratio, ε_e, is 230, while the Aestus nominal one has a value of 84. The reason is that no geometric restriction has been applied in this case, and the optimum point is a compromise solution between:

- The specific impulse: as the ε_e increases, I_{sp} grows, and consequently the propellant mass flow decreases for a constant E. Finally, considering the same burning time, it results in a lower M_{prop}
- The nozzle mass increases with the divergent area ratio due to its bigger size

The conclusion is that a geometric limitation is necessary in order to obtain an optimized engine, which can be installed in a concrete space launcher. Knowing that the Aestus components' distribution and the diameter of the Aestus cowling (5.5 m), the following restriction has been implemented:

$$D_{red,ta} + D_{ox,ta} + D_e < 4.5$$

That is, the sum of the fuel and oxidizer tank diameter, plus the nozzle exit diameter lets half meter of free space at each side of the engine for structure installation.

On the other hand, the three local optimized points don`t imply a global optimum. The next step is to find the optimum in two design parameters at the same time.

As it has been seen, the two best approximations to the Aestus engine have been achieved with the mixture ratio and nozzle area ratio optimization. For this reason, the minimum total vehicle mass is analyzed with the two previous design parameters, considering the nominal value of the injection pressure.

The iterations with different values of MR and ε_e are done automatically by the SQP solver (Sequential Quadratic Programming) included in the EcosimPro toolkit. The minimum total vehicle mass results 16943Kg, which is based on the following rocket design parameters:

Optimum with two variables	
Injection pressure, P_{inj}	11.4 bar
Mixture ratio, MR_{opt}	1.74
Nozzle area ratio, $\varepsilon_{e,opt}$	85.4

The result is a fairly Aestus rocket engine, which is an indication of the proper modeling of the three design modules. The main differences in performance, size and weight between the previous rocket design and the Aestus is detailed in the following table:

Parameter	Optimum x2	Aestus
Isp, m/s	3178	3143.5
D_{throat}, m	0.135	0.135
M_{prop}, kg	9479	9628
M_0, kg	16943	17086

Finally, the complete model has been solved with the three design parameters: P_1, MR and ε_e. As a result of the design convergence (see *Figure 11*), it has been proved that a rocket design point exists.

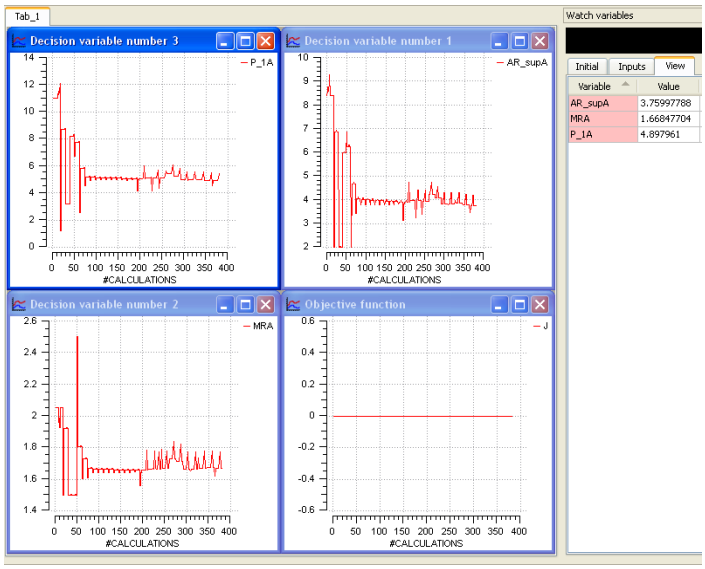

Figure 11. Iteration sequence of the three normalized design parameters looking for the minimum total vehicle mass

The minimum total vehicle mass results 16484Kg, which is based on the following rocket design parameters:

Optimum with three variables	
Injection pressure, $P_{inj,opt}$	4.9 bar
Mixture ratio, MR_{opt}	1.67
Nozzle area ratio, $\varepsilon_{e,opt}$	37.6

The resulting injection pressure is much lower than the Aestus nominal one. As it has been seen in the local optimization with the injection pressure, some empirical facts exceed the applied combustion model.

The main differences in performance, size and weight between the full rocket design and the Aestus is detailed in the following table:

Parameter	Optimum x3	Aestus
Isp, m/s	3073.5	3143.5
D_{throat}, m	0.204	0.135
M_{prop}, kg	9425	9628
M_0, kg	16484	17086

Note that if it could be possible to work with P_{inj} equal to 4.9 bar, the engine system would be 602 kg lighter.

B) Transient analysis of the designed engine

The components already programmed in the ESPSS libraries let compose a schematic to simulate the start, burning and stop of a rocket engine. Moreover, the new component momentum has been added in order to guarantee the desired perigee maneuver:

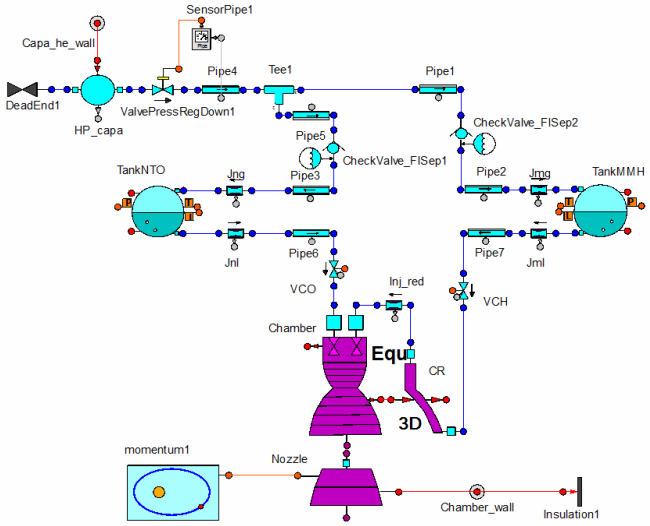

Figure 12. Transient Rocket Engine Model

Each of these components needs to know the value of some design parameters, such as the fuel tank volume and the throat diameter. These parameters are obtained from different sources:

- Mainly, the data determined by the preliminary design model, that is, the propulsion characteristics and the sizing&mass
- In addition, a simplified analysis must be taken in order to calculate some parameters. For example, the effective area of each injector system (fuel and oxidizer) is based on the continuity and linear momemtum equations:

$$\dot{m} = \rho \cdot A \cdot v$$

$$\Delta p = \xi \frac{1}{2} \rho \cdot v^2 = \frac{1}{C_d} \frac{1}{2} \rho \cdot v^2$$

Where $\dot{m}$ is the mass flow, ρ is the density, A is the effective area, and v is the flow velocity of the fuel

or oxidizer. Each fuel and oxidizer mass flow is supposed to need a pressure loss in the injection cavity and injectors of 20% of the chamber pressure. And the injectors are characterized with the discharge coefficient, C_d, which has usually a value of 0.7

- Finally, the engine control system must be defined in order to know the sequence of ignition and stop. For example, it has the responsibility to say when and how the valves must be opened

The main objective of this transient analysis is to guarantee the requirements given to the preliminary design, such as:

a) *The propellant level at the tanks.* It allows checking if the reserve fuel matches up with the percentage of total fuel given as data in the preliminary design (*Figure 13*)

b) *The trajectory during the maneuver.* The engine ignition takes place at the intersection between the circular initial orbit (h=250km) and the horizontal axis (y=0m). As it can be seen, there is a significant difference between this quasi-elliptical trajectory and the Hohmann ideal maneuver, due to a finite burning time of approximate 17 minutes (*Figure 14*)

c) *The temporal evolution of the design variables.* For example, the overpressure at the engine start must be under control, in order to avoid combustion instabilities and the burst of the combustion chamber (*Figure 15*)

d) *The temporal evolution of the propulsion characteristics.* One of the hypotheses made along the model is that thrust is constant during the burning. As it can be seen at the following picture, the transient simulation confirms that the thrust is almost the same in the whole combustion range (*Figure 16*)

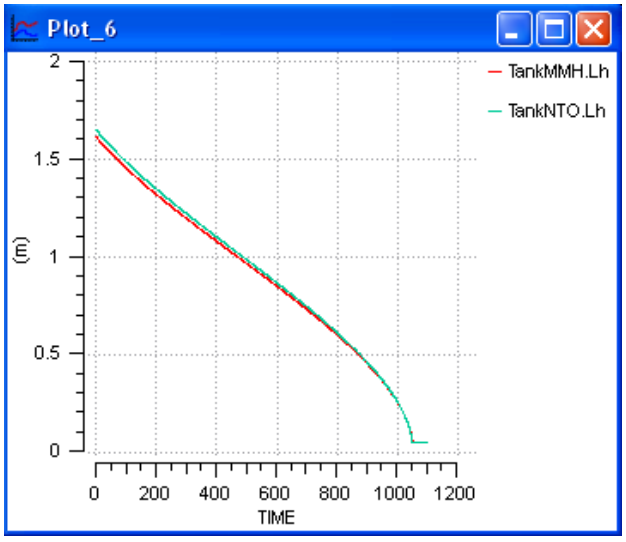

Figure 13. Fuel and oxidizer tanks' level

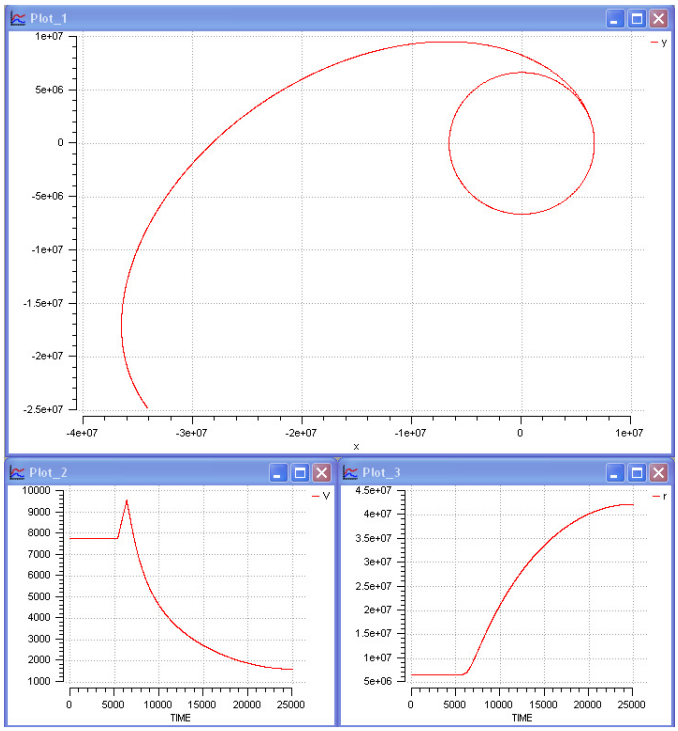

Figure 14. Resulting perigee manoeuvre (rocket position in its transfer plane, velocity profile and radius profile)

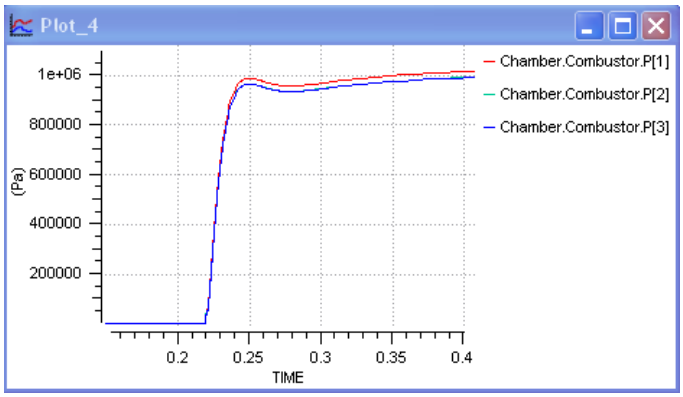

Figure 15. Combustion pressure at different combustor sections

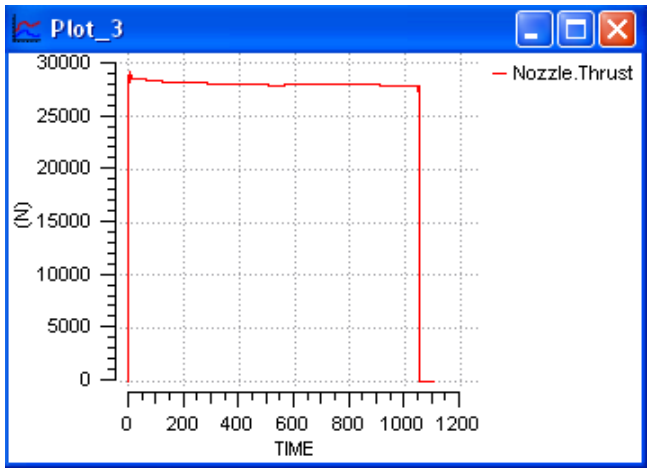

Figure 16. Thrust profile during the maneuver

9. CONCLUSSIONS

Developed ESPSS sub-models for the design of a liquid propellant rocket engine have been successfully tested and compared with the Aestus real engine.

These models have been coupled with an external optimizer, which determines the design parameters (chamber pressure, mixture ratio and nozzle area ratio) looking for the minimum initial vehicle mass. So that, given the mission requirements and cycle specifications, a complete rocket engine is sized.

Finally, a transient ESPSS model integrating the design parameters has been run in order to validate the design models. The obtained transient performances show good agreement with the requirements imposed in the design problem.

This study is focused on pressurized rocket engines, but it have been verified that these models can be easily extended to other cycles (e.g. expander cycles).

Nomenclature

η	Efficiency	-
ρ	Density	kg m^{-3}
ξ	Pressure drop coefficient	-
Δv	Maximum change of speed	m/s
A	Flow area	m^2
ε_e	Nozzle area ratio	-
ε_{ch}	Chamber / throat area ratio	-
c*	Characteristic velocity	m/s
c_E	Thrust coefficient	-
D	Diameter	m
F	Thrust	N
g	Standard gravity	m/s^2
h_t	Total specific enthalpy	J kg^{-1}
I_{sp}	Specific impulse	m/s
M	Mass	kg
m	Mass flow rate	kg s^{-1}
MR	Mixture ratio	-
n	Vehicle acceleration in g's	-
P	Pressure	Pa
R	Specific gas constant	J kg^{-1} K^{-1}
s	Entropy	J kg^{-1} K^{-1}
T	Temperature	K
t	time	s
v	Fluid speed	m s^{-1}
y	Molar fraction	-

Subindex

0	Initial
1	Injection section
2	Cylindrical chamber exit
b	Burning
cc	Combustion chamber
cr	Critical conditions
th	Throat
oxi	Oxidizer propellant
pg	Pressurized gas
PL	Payload
prop	Propellant
red	Reducer propellant
vac	Vacuum

References

1 http://www.ecosimpro.com

2 Moral, J.; Pérez, R.; Steelant, J.; de Rosa, M.; ESPSS Simulation Platform, Empresarios Agrupados Int., 2010

3 Manski, D.; Martin, J.A.; Optimization of the Propulsion Cycles for Advanced Shuttles. Part 1: Propulsion Mass Model Methodology, AIAA-89-2279, 25th Joint Propulsion Conference, 1989

4 Gordon, S.; McBride, B.J.; Computer Program for Calculation of Complex Chemical Equilibrium Compositions and Applications – I. Analysis, NASA Reference Publication 1311, 1994

5 Humble; Henry; Larson, Space Propulsion Analysis and Design, Mc Graw-Hill 1995

6 Sutton G.P., Rocket Propulsion Elements, 6th edition, John Wiley & Sons, Inc. 1992

7 Salvá, J.J.; Apuntes de Motores Cohete, ETSIA-UPM 2010

8 Manski, D.; Martin J.A., Evaluation of Innovative Rocket Engines for Single-stage Earth-to-orbit Vehicles, Journal of Propulsion, vol. 7, NO. 6, Nov.-Dec. 1991

9 Chobotov, V.A.; Orbital Machanics, Third Edition, AIAA Education Series 2002

10 E. Pérez et al., Ariane 5 User's Manual, Arianspace, 2008